

# Thermal Decomposition and Safety Assessment of N-Nitrodihydroxyethyl Dinitrate by DSC and ARC

Jun Zhang, Yingying Ma, Shuxin Chen, Liping Chen, and Wanghua Chen

**Abstract**—N-Nitrodihydroxyethyl dinitrate (DINA), an explosive as well as high-energy plasticizer, was widely used in double-base propellant production. In this paper, the thermal explosion hazard and decomposition progress of DINA under dynamic and adiabatic conditions were investigated using differential scanning calorimeter (DSC) and accelerating rate calorimeter (ARC) respectively to acquire thermodynamic parameters (e.g.  $T_{\text{onset}}$ ,  $T_p$  and  $\Delta H_d$ ) for self-heat reactions. The specific heat capacity was calculated based on a linear ramp method using DSC. Furthermore, we carried out these tests, which can provide more useful information for determining the decomposition kinetic parameters ( $E_a$  and  $A$ ) and thermal hazard parameters ( $\Delta G^\ddagger$ ,  $\Delta H^\ddagger$ ,  $\Delta S^\ddagger$ ,  $T_b$  and  $T_{D24}$ ) under the non-isothermal and adiabatic conditions, respectively. The SADT predictions for the 5, 20 and 50 kg packages of DINA and some simulation for spatial distribution of  $T$  and  $\alpha$  have been performed using the finite element analysis method of AKTS software, which can help us to optimize the conditions of storage and transportation for chemical, also minimize industrial disasters.

**Index Terms**—N-Nitrodihydroxyethyl dinitrate, DSC, ARC, Thermal decomposition kinetic, Hazards assessment.

## I. INTRODUCTION

N-Nitrodihydroxyethyl dinitrate (DINA), an explosive as well as high-energy plasticizer, was widely used in double-base propellant production. Its explosive performance is similar to that of RDX [1]. DINA as a high-energy plasticizer added to the propellant not only improves the solubility of the high-nitrogen nitrocellulose, but also facilitates the plasticization of the chemicals. It's beneficial for energy increase and ablation reduction for composite explosive, due to its advantages over nitroglycerin: higher energy, larger specific volume, lower combustion temperature and the high capability to plasticize and solve the high nitrogen content nitrocellulose.

At the end of last century, systematic research on the energetic material DINA have been carried out. Overviewing the research results, it is mainly focused on the development and optimization of the synthetic process of the material [2]. Although a small amount of literature has previously studied the thermal decomposition characteristics and kinetics of DINA, little work has been done for

determining on which the physicochemical properties and the thermal hazard parameters, especially for the calculation of exothermic properties and thermal explosion performance parameters of high-energy compounds [3]-[5]. It is important to research the thermal explosiveness of a reactive chemical in order to ensure safe operation, storage and transportation.

In this paper, the thermal explosion hazard and decomposition progress of DINA were investigated by DSC and ARC to acquire thermodynamic parameters (e.g.  $T_{\text{onset}}$ ,  $T_p$  and  $\Delta H_d$ ) for self-heat reactions. The specific heat capacity was calculated based on a linear ramp method using DSC. Furthermore, we carried out these tests, which can provide more useful information for determining the decomposition kinetic parameters ( $E_a$  and  $A$ ) and thermal hazard parameters ( $\Delta G^\ddagger$ ,  $\Delta H^\ddagger$ ,  $\Delta S^\ddagger$ ,  $T_b$  and  $T_{D24}$ ) under the non-isothermal and adiabatic conditions, respectively. The SADT predictions for the 5, 20 and 50 kg packages of DINA and some simulation for spatial distribution of  $T$  and  $\alpha$  have been performed using the finite element analysis method of AKTS software, which can help us to optimize the conditions of storage and transportation for chemical, also minimize industrial disasters [6], [7].

## II. EXPERIMENTAL

### A. Materials

N-Nitrodihydroxyethyl dinitrate used in the tests is an industrially pure white crystal, provided by Liaoning Qingyang Chemical Industry Group Co., LTD. Fig. 1 shows the constructed chemical molecular structure of DINA by Chemdraw software 16.0.

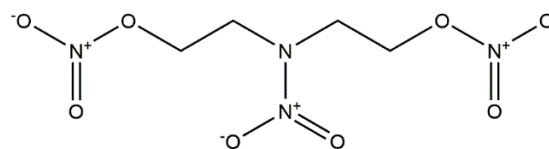


Fig. 1. Constructed chemical molecular structure of DINA.

### B. Apparatus and Test Conditions

#### 1) DSC experiments

DSC is a popular thermal analysis instrument. It can be used to study thermal stabilities and decomposition characteristics of materials, especially for hazardous materials [8-10]. The DSC used in this paper was manufactured by METTLER TOLEDO (DSC-1).

Calorimetric sensitivity: 0.04  $\mu$ W;

Test temperature range: -35  $^{\circ}$ C ~ 500  $^{\circ}$ C;

Heat flow detection range:  $\pm$  350mW.

Manuscript received February 3, 2020; revised April 20, 2020.

Jun Zhang, Shuxin Chen, Liping Chen, and Wanghua Chen are with the Department of Safety Engineering, School of Chemical Engineering, Nanjing University of Science & Technology, No.200, Xiaolingwei Road, Xuanwu District, Nanjing 210094, China (e-mail: {799339229@qq.com, 932164927@qq.com, clp2005@hotmail.com, chenwh\_nust@sina.com}).

Yingying Ma is with Solvay (China) Co., Ltd., Shanghai 201108, China (e-mail: mayingying100@gmail.com).

Stainless steel high-pressure crucibles (30 $\mu$ l) with gold-plated pads were used as test cells, which can bear a pressure of 15 MPa, and an empty one was used as the reference.

The tests for determining the specific heat capacity, which select the mass of test sample (DINA) and standard sample (sapphire) were both 20mg, and tested at the heating rate of 5 $^{\circ}\text{C}\cdot\text{min}^{-1}$  over the temperature range of 20 $^{\circ}\text{C}$ -110 $^{\circ}\text{C}$ .

During dynamic DSC experiments, DINA was tested at four heating rates of 2  $^{\circ}\text{C}\cdot\text{min}^{-1}$ , 4  $^{\circ}\text{C}\cdot\text{min}^{-1}$ , 8  $^{\circ}\text{C}\cdot\text{min}^{-1}$  and 10  $^{\circ}\text{C}\cdot\text{min}^{-1}$  respectively over the temperature range of 25 $^{\circ}\text{C}$ -380  $^{\circ}\text{C}$ , and the sample mass were (0.9  $\pm$  0.01) mg; High-purity nitrogen (99.999%) was regarded as shielding gas (200 ml  $\text{min}^{-1}$ ) and purge gas (50 ml  $\text{min}^{-1}$ ).

## 2) ARC experiments

ARC, manufactured by Thermal Hazard Technology Company (es-ARC), is a popular and efficient apparatus to test the thermal behavior under adiabatic condition.

Test temperature range: Room temperature  $\sim$  500  $^{\circ}\text{C}$ ;

Test pressure range: 0-15 MPa;

Detection sensitivity: 0.02  $^{\circ}\text{C}\cdot\text{min}^{-1}$ ;

Test mode: H-W-S (heat-wait-seek);

Heating step: 5  $^{\circ}\text{C}$ ;

Waiting time: 15 min;

DINA was tested using Ti-LCQ bomb (10ml, 7.185g) in 80 $^{\circ}\text{C}$ -280 $^{\circ}\text{C}$ , and with mass of 0.115 g.

## III. RESULTS AND DISCUSSION

### A. Calculation of Specific Heat Capacity

The specific heat capacity of DINA was measured based on a linear ramp method using DSC. We can regard the heat flow rate as a function of temperature, then determine a function of the specific heat capacity with temperature:

$$C_p(T) = \frac{dH(T)}{dT} \times \frac{1}{m} \quad (1)$$

where  $C_p$  is the specific heat capacity,  $\text{J g}^{-1} \text{K}^{-1}$ ;  $H$  is enthalpy, J;  $T$  is temperature, K;  $m$  is sample mass, g.

In practice, it is difficult to determine the value of enthalpy precisely because of the limitation of an instrument itself and the operating conditions. So, an indirect procedure is used to calculate  $C_p$  value of the sample using DSC where three DSC scans are necessary—scan of baseline, standard material (sapphire) and sample (DINA). This indirect procedure can be done in two ways, as continuous method or as stepwise method [11]-[14]. In both methods, the temperature profile starts and ends by an isotherm. These isotherms are necessary to arrange all three curves for evaluation—isotheim should overlap in all three curves.

All three tests were operated in stepwise method, which is based on comparison of areas under DSC curves obtained for standard and the sample according to equation:

$$C_p(T) = \frac{m_{\text{std}}}{m_s} \times \frac{DSC_s(T) - DSC_{\text{bl}}(T)}{DSC_{\text{std}}(T) - DSC_{\text{bl}}(T)} \times C_{p_{\text{std}}} \quad (2)$$

where  $DSC$  is the heat flow at the temperature  $T$ ,  $\mu\text{W}$ ; Subscripts “s”, “std” and “bl” corresponding to DINA, sapphire and baseline, respectively.

The stepwise method was tested using single step measurements. 15 minutes of isotherm on the beginning and 10 minutes at the end of step were sufficient to reach equilibrium as is seen in Fig. 2.

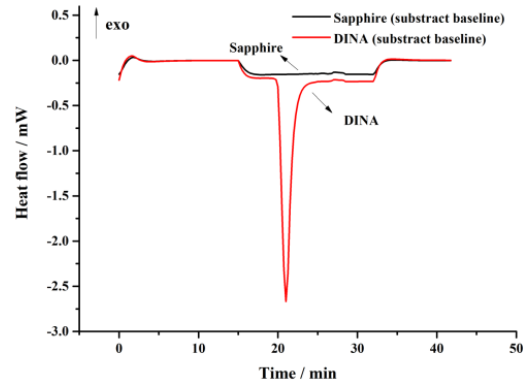


Fig. 2. Stepwise method performed at heating rate 5  $^{\circ}\text{C}\cdot\text{min}^{-1}$ .

As seen from Fig. 2, we can find that in the process of test, the onset endothermic temperature of DINA is about 50 $^{\circ}\text{C}$ . It can be considered that the endothermic peak corresponds to the melting process of the sample, with reference to the literature value of melt point for DINA is 50  $^{\circ}\text{C}$ . As the sample underwent a melting phase transition, its specific heat capacity is catastrophically unstable and generally not considered. Considering that the  $C_p$  of the sample changed after the phase transition, the  $C_p$  under the solid and liquid phases have been calculated separately. Therefore, the heat release data of DINA under the corresponding phase state have been selected to calculate the  $C_p$  (based on the DIN51007 method). The calculation results have been shown in Fig. 3(a) and Fig. 3(b).

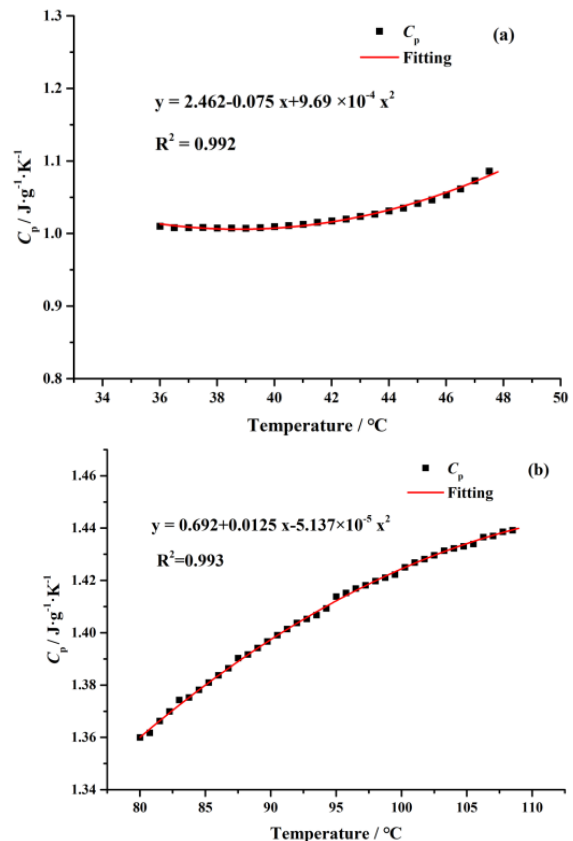


Fig. 3. Calculation results of  $C_p$  ((a)-Solid state, (b)-Liquid state).

Solid state:  $C_p(T) = 2.462 - 0.075 \times (T - 273.15) + 9.69 \times 10^{-4} \times (T - 273.15)^2$  ( $30^\circ\text{C} \leq T \leq 50^\circ\text{C}$ )  
 Liquid state:  $C_p(T) = 0.692 + 0.0125 \times (T - 273.15) - 5.137 \times 10^{-5} \times (T - 273.15)^2$  ( $80^\circ\text{C} \leq T \leq 110^\circ\text{C}$ )

### B. Dynamic DSC Experiments

#### 1) Experimental results and analysis

Fig. 4 shows the different heat flow curves for DINA under different heating rates, and the corresponding thermodynamic data have been listed in Table I.

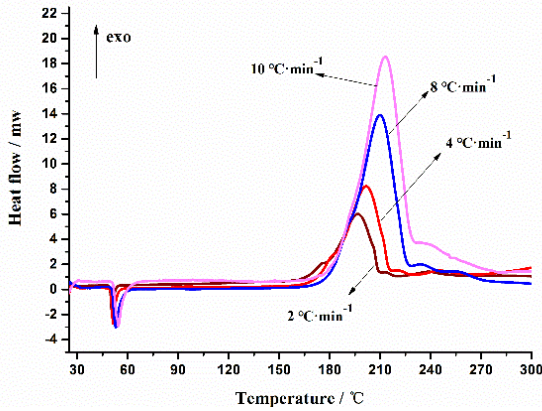


Fig. 4. Heat flow curves of DINA under different heating rates.

TABLE I: DYNAMIC DSC RESULTS OF DINA

Sample data		DSC experiment (STARe programmed)				
		Endothermic process		Exothermic process		
$\beta / ^\circ\text{C min}^{-1}$	$m / \text{mg}$	$T_{\text{melt}} / ^\circ\text{C}$	$T_{p1} / ^\circ\text{C}$	$T_{\text{onset}} / ^\circ\text{C}$	$T_{p2} / ^\circ\text{C}$	$\Delta H_d / \text{J g}^{-1}$
2	1.00	49.47	50.69	153.95	196	3329
4	1.01	49.86	51.38	156.88	201	3175
8	1.00	50.62	52.78	159.54	209	3148
10	1.00	51.32	53.40	162.50	213	3288

The dynamic DSC results shown in Fig. 4 and Table I reveal that in the process of test, the endothermic peak and exothermic peak of DINA are identified at about  $50\text{--}53^\circ\text{C}$  and  $153\text{--}162^\circ\text{C}$ , respectively. And then a sharp exothermic decomposition start to take place at about  $180^\circ\text{C}$ , which is similar to the results in Ref. [1]. As the heating rate increased, the exothermic peak moved to the high temperature region, which made the onset decomposition temperature ( $T_{\text{onset}}$ ) and the peak temperature all increased.

The average decomposition enthalpy for the four experiments is approximately  $3235.63 \text{ J g}^{-1}$ , which was greater than  $800 \text{ J g}^{-1}$ . According to the discriminating conditions of the literature [15], once the decomposition reaction occurs, the severity of the accident is great.

#### 2) Calculations of thermodynamic and kinetic parameters

To determine the dynamic decomposition kinetic parameters of energetic materials, the Kissinger's method [16] has been employed. The peak temperature of corresponding exothermic peaks was obtained based on DSC curves of four different heating rates, then to determine the decomposition kinetic parameters of the sample. The Kissinger's equation was defined as following:

$$\ln \frac{\beta}{T_p^2} = \ln \frac{RA}{E_a} - \frac{E_a}{RT_p} \quad (3)$$

where  $\beta$  is heating rates,  $^\circ\text{C} \cdot \text{min}^{-1}$ ;  $T_p$  is peak temperature, K;  $R$  is a universal gas constant,  $8.314 \text{ J mol}^{-1} \text{ K}^{-1}$ ;  $A$  is pre-exponential factor,  $\text{min}^{-1}$ ;  $E_a$  is apparent activation energy,  $\text{kJ mol}^{-1}$ .

In the Kissinger's method, the left side of equation (3) is plotted against  $1/T_p$  giving rise to a straight line (Fig. 5) whose slope yields the activation energy, further to determine the value of pre-exponential factor, and the calculation results have been listed in Table II.

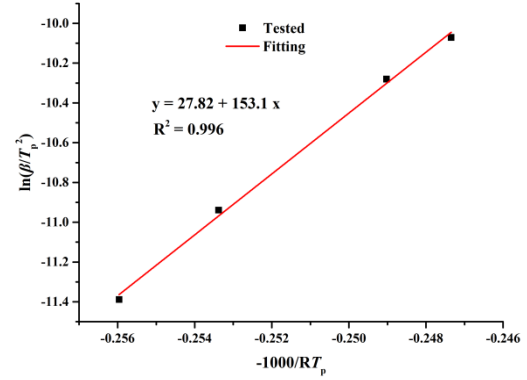


Fig. 5. Calculation results of thermal kinetic parameters based on dynamic DSC data.

According to following Eqs. (4), (5) and (6), we can determine the free energy of activation ( $\Delta G^\ddagger$ ), activation enthalpy ( $\Delta H^\ddagger$ ), and activation entropy ( $\Delta S^\ddagger$ ) at peak temperature in the exothermic decomposition process corresponding to  $\beta \rightarrow 0$  ( $T_{p0}$ ) can be calculated by Eq. (7) [17].

$$A \exp\left(-\frac{E_a}{RT}\right) = \frac{k_B T}{h} \exp\left(-\frac{\Delta G^\ddagger}{RT}\right) \quad (4)$$

$$\Delta H^\ddagger = E_a - RT \quad (5)$$

$$\Delta G^\ddagger = \Delta H^\ddagger - T\Delta S^\ddagger \quad (6)$$

$$T_{pi} = T_{p0} + a\beta_i + b\beta_i^2 \quad i=2, 4, 8 \text{ and } 10 \quad (7)$$

where  $k_B$  is a Boltzmann constant,  $1.3807 \times 10^{-23} \text{ J K}^{-1}$ ;  $h$  is a Planck constant,  $6.625 \times 10^{-34} \text{ J s}$ ;  $T_{pi}$  is the peak temperature of a heating rate of  $\beta_i$ ;  $a$  and  $b$  are the coefficients.

#### The critical temperature of thermal explosion ( $T_b$ )

Another critical thermodynamic parameter, the critical temperature of thermal explosion in the exothermic decomposition process corresponding to  $\beta \rightarrow 0$  ( $T_{bp0}$ ), which can be calculated using Zhang-Hu-Xie-Li Eq. (8) applied in the National Military Standard of the People's Republic of China—GJB772A-97.

$$T_{bp0} = \frac{E_a - \sqrt{E_a^2 - 4E_a RT_{bp0}}}{2R} \quad (8)$$

All these calculated thermodynamic and kinetic parameters have been listed in Table II.

### C. ARC Experiments

In order to be able to further understand the thermal decomposition and the kinetic parameters of DINA, after obtaining the parameters under the dynamic DSC tests, an adiabatic test (ie, ARC test) should also be performed to obtain the decomposition performance parameters of DINA under adiabatic condition.

TABLE II: KINETIC AND THERMODYNAMIC PARAMETERS OF DINA

Parameters	$E_a$	$\ln A$	$T_{p0}$	$\Delta G^\ddagger$	$\Delta H^\ddagger$	$\Delta S^\ddagger$	$T_{bp0}$	a	b
	$\text{kJ mol}^{-1}$	$\text{min}^{-1}$	$^\circ\text{C}$		$\text{kJ mol}^{-1}$		$^\circ\text{C}$		
Calculation	153	37.6	188	139.1	149.3	22	200	3.7	-0.12

### 1) Experimental results and analysis

As we seen in Figs. 6a and b, there are some curves of temperature and pressure vs. time and self-heating rate vs. temperature during exothermal stage, which were obtained in adiabatic experiments. It is found from Fig. 6a that the thermal decomposition of DINA began at 135.28°C. The pressure increased non-linearly as the temperature increased during the decomposition process, and there was a dramatically increase of  $dP/dt$  and  $dT/dt$  when the temperature exceeded 162 °C. The temperature and pressure of reaction system jumped from 162 °C (5.6bar) to 200 °C (11.2bar) during just 25 minutes, which confirmed that the decomposition reaction released enormous energy and could cause a disaster when occurred uncontrolled in a closed vessel.

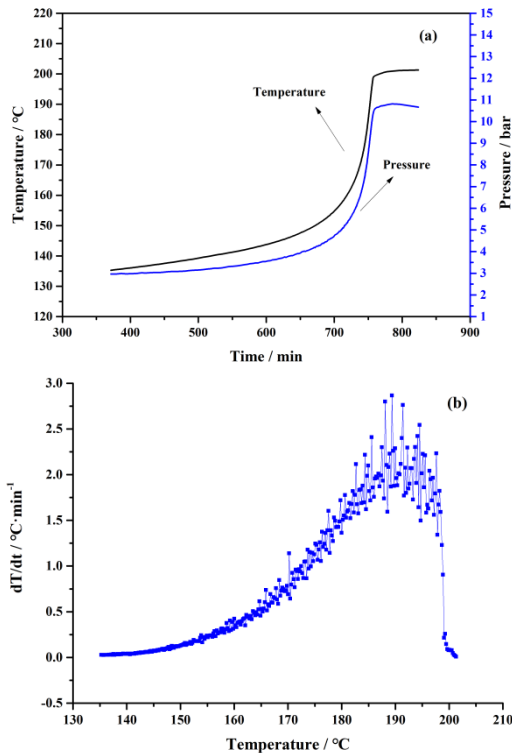


Fig. 6. Curves of adiabatic test during exothermal stage ((a)-T and P vs. time, (b)-SHR curve).

### 2) Calculation of gas production

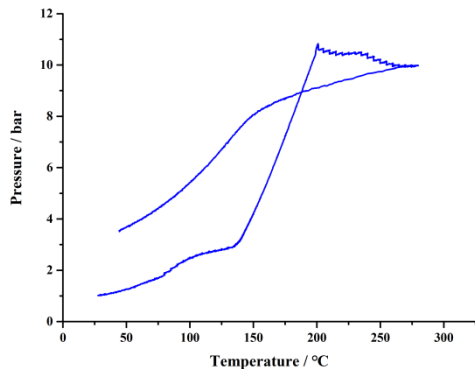


Fig. 7. Curve of pressure vs. temperature during the whole test.

According to the results shown in Fig. 7, the pressure corresponding to 50 °C (323.15 K) at the beginning of the tests ( $P_0$ ) was considered as a reference during the calculation, and  $P_1$  represented the corresponding pressure as the test was stopped and cooled to 50 °C.

Initial conditions:  $P_0 = 1.27$  bar;  $T_0 = 323.15$  K; Amount of substance at the beginning of the test ( $n_0$ ).

Final conditions:  $P_1 = 3.69$  bar;  $T_1 = 323.15$  K; The volume of gas production,  $V_b \approx 10$  ml; Amount of substance at the end of the test ( $n_1$ ).

According to the Ideal Gas Law:

$$\Delta n = n_1 - n_0 = \frac{P_1 - P_0}{P_0} n_0 \quad \text{Gas production} \quad (9)$$

Under ideal conditions (1.01325 bar, 298.15 K), the volume of gas production ( $V$ ) and the amount of substance ( $n$ ) can be determined using following equations:

$$V = \frac{T(P_1 - P_0)V_b}{PT_1} = \frac{298.15 \times (3.69 - 1.27) \times 10}{323.15 \times 1.01325} = 22.04 \text{ ml} \quad (10)$$

$$n = \frac{(P_1 - P_0)V_b}{RT_0} = \frac{(3.69 - 1.27) \times 10^{-5} \times 10 \times 10^{-6}}{8.314 \times 323.15} = 9.0 \times 10^{-4} \text{ mol} \quad (11)$$

Therefore, the calculation results for total gas production have been determined as follow:

$$\frac{n}{m} = \frac{9.0 \times 10^{-4}}{0.115} = 0.0078 \text{ mol} \cdot \text{g}^{-1} = 7.8 \text{ mol} \cdot \text{kg}^{-1} \quad (12)$$

Several adiabatic decomposition parameters have been calculated using ARCCAL program [18], and now are listed in Table III.

TABLE III: ADIABATIC DECOMPOSITION PARAMETERS OF DINA

Decomposition parameters	ARC experiment data (ARCCAL programmed)	
	Experiment data	Corrected values
m / g	0.115	—
Onset temperature / °C	135.28	117.25
Onset temperature rate / °C · min <sup>-1</sup>	0.027	0.474
Max rate temperature / °C	189.35	1066.56
Max temperature rise rate / °C · min <sup>-1</sup>	2.866	50.32
Final temperature / °C	201.32	1276.71
Phi-factor	17.557	—
Adiabatic temperature rise / °C	66.04	1159.46
Total gas production / mol kg <sup>-1</sup>	7.8	—

### 3) Data correction

Under experiment conditions of ARC, heat from the exothermic reaction of the sample induced the temperature rise of both the sample and the reaction cell. Since the sample tested by ARC is in a non-ideal adiabatic environment, the thermal inertia factor  $\phi$  is required to correct the test results. The correction calculation is performed as following [18]-[20]:

$$\phi = 1 + \frac{M_b C_{vb}}{M_s C_{vs}} \quad (13)$$



$$T_{0,corr} = \left( \frac{1}{T_0} + \frac{R}{E_a} \ln \phi \right)^{-1} \quad (14)$$

$$T_{m,corr} = T_{0,corr} + \phi(T_m - T_0) \quad (15)$$

$$\Delta T_{ad,corr} = \phi \Delta T_{ad} \quad (16)$$

$$T_{f,corr} = \Delta T_{ad,corr} + T_{0,corr} \quad (17)$$

$$m_{corr} = \phi m \quad (18)$$

where  $M_s$ ,  $M_b$  are the mass of sample and test cell, g;  $C_{vs}$ ,  $C_{vb}$  are the heat capacity of sample and test cell,  $J g^{-1} K^{-1}$ ;  $m$  is the temperature rise rate,  $K min^{-1}$ ; The subscripts “0”, “m”, “f” and “corr” corresponding to the initial values, the values at the maximum rate, the final and corrected values, respectively.

#### 4) Kinetic calculations based on ARC data

After obtained the thermal decomposition parameters of DINA under the adiabatic conditions, we can process the ARC data based on the adiabatic kinetic model of the Townsend method. The Townsend method considers that the relationship between temperature rise rate and temperature in adiabatic conditions should be:

$$\frac{dT}{dt} = A \left( \frac{T_f - T}{\Delta T_{ad}} \right)^n C_0^{n-1} \Delta T_{ad} \exp \left( \frac{-E}{RT} \right) \quad (19)$$

Rearranging Eq. (16), we had:

$$k^* = k C_0^{n-1} = C_0^{n-1} A \exp \left( \frac{-E}{RT} \right) = \frac{dT}{dt} \left( \frac{\Delta T_{ad}}{T_f - T} \right)^n \Delta T_{ad}^{-1} \quad (20)$$

$$\ln k^* = \ln(A C_0^{n-1}) - \frac{E}{RT} \quad (21)$$

where  $k^*$  is a pseudo-zero-order rate constant at the temperature  $T$ ;  $t$  is the time, min;  $\Delta T_{ad}$  is the adiabatic temperature rise, K;  $n$  is reaction order;  $C_0$  is the initial concentration of DINA ( $6.6875 \text{ mol l}^{-1}$ ).

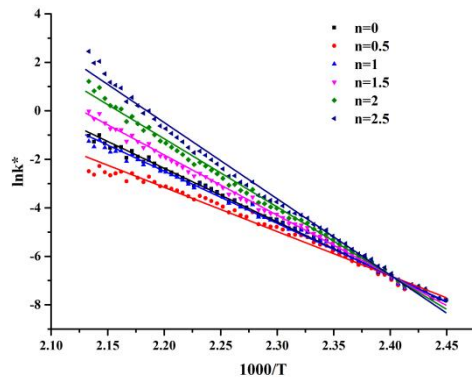


Fig. 8. Curves of  $\ln k^*$  vs.  $1/T$  for the self-heating decomposition of DINA.

TABLE IV: CALCULATION RESULTS OF KINETIC PARAMETERS BASED ON THE ARC DATA

Kinetic parameters	$E_a / \text{kJ mol}^{-1}$	$\ln A / \text{min}^{-1}$	$R^2$
$n = 0$	183.9	48.2	0.996
$n = 0.5$	151.6	37.9	0.988
$n = 1$	179.1	44.9	0.996
$n = 1.5$	206.6	51.8	0.998
$n = 2$	234.0	58.9	0.994
$n = 2.5$	261.5	65.9	0.989

The plot of  $\ln k^*$  vs.  $1/T$  is, therefore, expected to be a straight line providing that the order of reaction was correctly chosen. The curves between  $\ln k^*$  and  $1/T$  at

different  $n$  for the decomposition of DINA are illustrated in Fig. 8, the kinetic parameters ( $E_a$  and  $A$ ) and the corresponding linear correlation coefficient  $R^2$  could be determined from the plot also have been listed in Table IV.

Viewing to the kinetic calculation results shown in Table IV, we can know when the reaction order is 1.5, the linear coefficient of the kinetic calculation is the highest, which is 0.998. Therefore, we can believe that all kinetic parameters ( $n$ ,  $E$  and  $A$ ) of DINA were credible, they can be used for subsequent calculations.

#### The time to maximum rate under adiabatic conditions (TMR<sub>ad</sub>)

$T_{D24}$ , another important parameter for process risk assessment, was determined for DINA. It is the highest temperature at which the thermal stability of the reaction mass is unproblematic [21].

$$\ln \theta = \frac{E}{RT} - \ln A \quad (22)$$

$$\theta_{corr} = \theta / \phi \quad (23)$$

$\theta$  is the time to maximum temperature rate, s; The relationship between  $T$  and  $\theta$  was determined approximately using the Eq. (19). Due to the effect of thermal inertia, the actual TMR<sub>ad</sub> should be also corrected by  $\phi$  using Eq. (20). The results of calculating  $T_{D24}$  and  $T_{D8}$  using the above formula have been illustrated in Fig. 9.

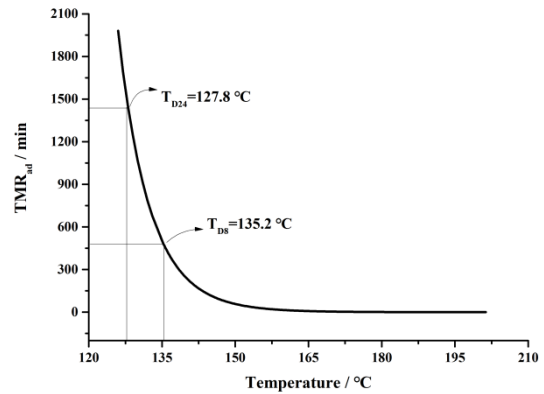


Fig. 9. Curves of TMR<sub>ad</sub> vs.  $T$  for DINA (corrected values).

#### D. Prediction of SADT Based on the Non-isothermal DSC Data

The self-accelerating decomposition temperature (SADT), an important parameter for characterizing thermal hazard possibility under transport conditions, is the lowest environmental temperature at which the temperature increment at least  $6^\circ\text{C}$  in a specified commercial package within 7 days or less. According to the recommendations on TDG, SADT is defined as “the lowest temperature at which self-accelerating decomposition may occur with a substance in the packaging as used in transport”. It can be determined by combining effect of decomposition kinetics, ambient temperature, heat transfer properties of the substance and its packaging.

AKTS software can deal with the tested data mathematically, which includes SADT prediction. It uses finite element analysis so that the temperature at any location within the package can be predicted at any given time [22].

In order to determine the SADT of DINA, the

non-isothermal decomposition kinetic parameters, the convective heat transfer from the package (the boundary conditions) as well as the conductive heat transfer within the package can now be introduced into calculating procedure. According to the criteria set by the United Nations SADT test H.4, for the 5, 20 and 50 kg packages of DINA, the cylinder-shaped packaging ( $H/D=2$ ) and sample parameters were applied:  $\rho$  ( $1600 \text{ kg m}^{-3}$ ),  $\lambda$  ( $0.1 \text{ W m}^{-1} \text{ K}^{-1}$ ),  $U$  ( $5 \text{ W m}^{-2} \text{ K}^{-1}$ ). The resulting temperature profile (the green curve represents the center of the package while the black curve represents the reaction progress) for the 50 kg package of DINA is provided in Fig. 10.

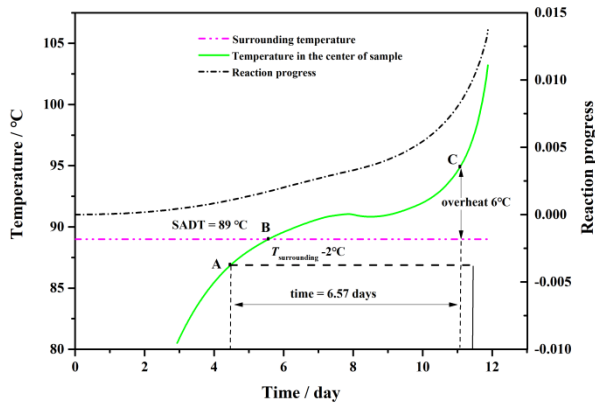


Fig. 10. Prediction of the SADT for 50 kg of DINA.

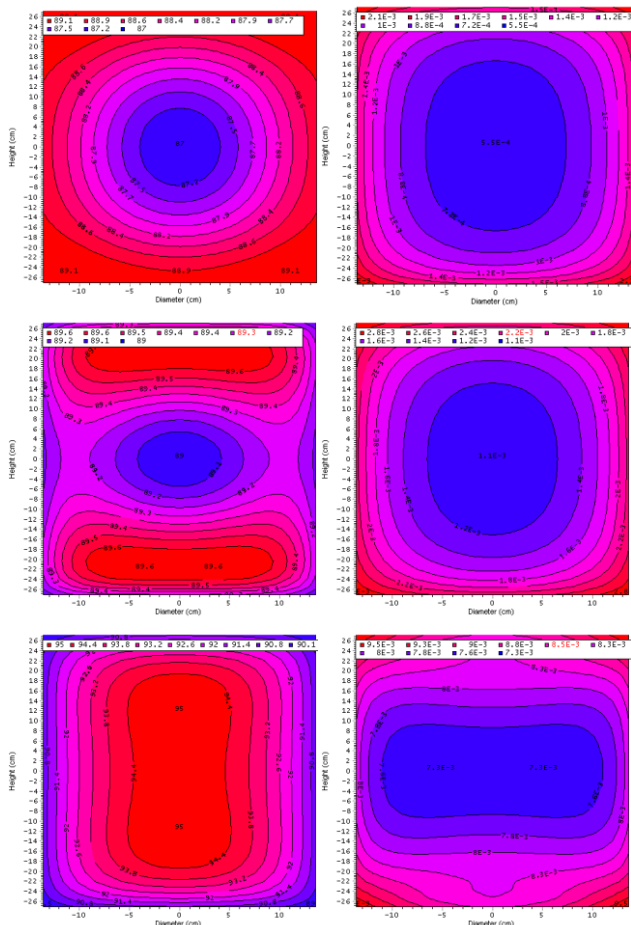


Fig. 11. Prediction of the spatial distribution of temperature (left) and reaction progress (right) for a mass of 50 kg in a cylinder with ratio  $H/D = 2$  after period of time—A (top), B (middle) and C (bottom).

Prediction based on the kinetic parameters determined

from dynamic DSC signals indicate that a temperature of  $89^\circ\text{C}$  is the lowest environment temperature at which the temperature increment at least  $6^\circ\text{C}$  in a specified commercial package within 7 days or less. This period is measured from the time when the centre temperature of sample reaches  $2^\circ\text{C}$  below the surrounding temperature (after ca. 4.47 days) (Point A). After about 5.55 days (Point B), the centre temperature is equal to the surrounding temperature. The overheat of  $6^\circ\text{C}$  occurs after about 11.04 days (Point C). Fig. 11 shows the simulated spatial distribution of the temperature (left column) and reaction progress (right column) in the cylinder after period of time represented by the points A, B and C i.e. when the center temperature differs by  $-2^\circ\text{C}$ ,  $0^\circ\text{C}$  and  $+6^\circ\text{C}$ , respectively compared to the surrounding temperature.

The SADT values of 5kg and 20kg packages during storage and transportation were predicted based on the same prediction method using AKTS software, which are  $92^\circ\text{C}$  and  $90^\circ\text{C}$ , respectively.

#### IV. CONCLUSIONS

The basic chemical or physical properties and the thermokinetic characteristics of DINA have been obtained by carrying out DSC and ARC tests, which could provide more information for determining the decomposition kinetic parameters and estimating some critical thermal hazard parameters, to optimize the conditions of storage and transportation for chemical, also minimize industrial disasters.

(1) According to the DIN51007 method, the specific heat capacity of DINA under solid state can be described as  $C_p(T) = 2.462 - 0.075 \times (T - 273.15) + 9.69 \times 10^{-4} \times (T - 273.15)^2$ . Whereas for liquid state,  $C_p(T) = 0.692 + 0.0125 \times (T - 273.15) - 5.137 \times 10^{-5} \times (T - 273.15)^2$ .

(2) The dynamic DSC results indicate that the endothermic and exothermic peaks of DINA are identified at about  $50\text{--}53^\circ\text{C}$  and  $153\text{--}162^\circ\text{C}$ , respectively. The average decomposition enthalpy  $\Delta H_d$  is about  $3235.63 \text{ J g}^{-1}$ , indicating a tragedy if it decomposes in bulk. The non-isothermal decomposition kinetic parameters ( $E_a$ ,  $A$ ) determined by the Kissinger's method and several thermal hazard parameters ( $\Delta G^\ddagger$ ,  $\Delta H^\ddagger$ ,  $\Delta S^\ddagger$  and  $T_{bp0}$ ) have been calculated, which are all listed in Table II.

(3) Under adiabatic conditions, the initial decomposition temperature of DINA is about  $135^\circ\text{C}$ , also there was a dramatically increase of  $dP/dt$  and  $dT/dt$  when the temperature exceeded  $162^\circ\text{C}$ . The total gas production of decomposition process is  $7.8 \text{ mol kg}^{-1}$ . Kinetic calculation performed using the Townsend method reveal that the apparent  $E_a$  and  $A$  under adiabatic condition are  $206.6 \text{ kJ mol}^{-1}$  and  $3.14 \times 10^{22} \text{ min}^{-1}$ , ( $n=1.5$ ). Two critical thermal hazard parameters ( $T_{D24}$  and  $T_{D8}$ ) corrected by  $\phi$  are calculated as  $127.8^\circ\text{C}$  and  $135.2^\circ\text{C}$ , respectively.

(4) Another critical parameter for thermal hazard assessment (SADT) have been predicted based on the non-isothermal decomposition kinetic parameters using AKTS software. Prediction results reveal that the SADT of the 5, 20 and 50 kg packages of DINA are  $92^\circ\text{C}$ ,  $90^\circ\text{C}$  and  $89^\circ\text{C}$ , respectively.

(5) Using the finite element analysis of AKTS software, we have simulated the spatial distribution of the temperature and reaction progress of DINA after period of time represented by the points when the center temperature differs by  $-2^{\circ}\text{C}$ ,  $0^{\circ}\text{C}$  and  $+6^{\circ}\text{C}$ , respectively compared to the surrounding temperature.

#### ACKNOWLEDGMENT

This investigation was financed by the National key R&D Program of China (2017YFC0804701-4). The authors thank for this support.

#### CONFLICT OF INTEREST

The authors declare no conflict of interest.

#### AUTHOR CONTRIBUTIONS

Jun Zhang conducted the research; Yingying Ma and Shuxin Chen analyzed the data; Jun Zhang wrote the paper; Liping Chen and Wanghua Chen revised the manuscript; All authors had approved the final version.

#### REFERENCES

- [1] Y. Y. Ma, "Effect of DINA on the performance of double base propellant," *Chinese Journal of Energetic Materials*, vol. 3, no. 2, pp. 31–36, 1995.
- [2] A. Ksiqczak, M. Ostrowski, and W. Tomaszewski, "Thermochemistry of the binary system nitrocellulose + N-nitrodiethanolamine dinitrate," *J. Therm. Anal. Calorim.*, vol. 94, pp. 275–279, 2008.
- [3] G. N. Rao, W. Feng, J. Zhang, S. Y. Wang, L. P. Chen, Z. C. Guo, and W. H. Chen, "Simulation approach to decomposition kinetics and thermal hazards of hexamethylenetetramine," *J. Therm. Anal. Calorim.*, vol. 8, pp. 1–10, 2018.
- [4] L. Zhao, Y. Yin, H. L. Sui, Q. Yua, S. H. Sun, H. B. Zhang, S. Y. Wang, L. P. Chen, and J. Sun, "Kinetic model of thermal decomposition of CL-20/HMX co-crystal for thermal safety prediction," *Thermochim. Acta*, vol. 674, pp. 44–51, 2019.
- [5] Y. T. Tsai, A. C. Huang, S. C. Ho, and C. M. Shu, "Potential explosion hazard of polyester resin dust formed from a granulation process: limiting oxygen concentration with different pressures," *Appl. Therm. Eng.*, vol. 135, pp. 74–82, 2018.
- [6] C. Yan, Z. Wang, K. Liu, Q. Zuo, Y. Zhen, and S. Zhang, "Numerical simulation of size effects of gas explosions in spherical vessels," *Simulation*, vol. 93, pp. 695–705, 2017.
- [7] C. R. Cao, S. H. Liu, M. Das, and C. M. Shu, "Evaluation for the thermokinetics of the autocatalytic reaction of cumene hydroperoxide mixed with phenol through isothermal approaches and simulations," *Process Saf. Environ. Prot.*, vol. 117, pp. 426–438, 2018.
- [8] B. Roduit, C. Borgeat, B. Berger, P. Folly, and H. Andres, "Up-scaling of DSC data of high energetic materials," *J. Therm. Anal. Calorim.*, vol. 85, no. 1, pp. 195–202, 2006.
- [9] G. Singh, D. K. Pandey, "Thermal studies on energetic compounds," *J. Therm. Anal. Calorim.*, vol. 76, no. 2, pp. 507–519, 2004.
- [10] S. M. Pourmortazavi, M. Rahimi-Nasrabadi, I. Kohsari, and S. S. Hajimirsadeghi, "Non-isothermal kinetic studies on thermal decomposition of energetic materials," *J. Therm. Anal. Calorim.*, vol. 110, no. 2, pp. 857–863, 2012.
- [11] G. Hohne and W. Hemminger, *Differential Scanning Calorimetry*, 2nd ed. Berlin: Springer-Verlag, 2003.
- [12] ASTM norm E1269-11: Standard Test Method for Determining Specific Heat Capacity by Differential Scanning Calorimetry, Pennsylvania, ASTM International.
- [13] *Application note M149-v1*, Setaram.
- [14] S. Mraw and D. Naas, "Measurement of accurate heat-capacities by differential scanning calorimetry comparison of DSC results on pyrite (100 to 800 K) with literature values from precision adiabatic calorimetry," *J. Therm. Anal. Calorim.*, vol. 11, pp. 567–584, 1979.
- [15] F. Stoessel, *Thermal Safety of Chemical Processes*, Weinheim: Wiley-VCH, pp. 279–282, 2008.
- [16] H. Kissinger, "Reaction kinetics in differential thermal analysis," *Analytical Chemistry*, vol. 29, no. 11, pp. 1702–1706, 1957.

- [17] F. Bao and G. Zhang, "Thermal decomposition and safety assessment of 3, 30-dinitrimino-5,50-bis(1H-1,2,4-triazole) by DTA and ARC," *J. Therm. Anal. Calorim.*, vol. 132, pp. 805–811, 2018.
- [18] G. Zhang and S. Jin, "Thermal hazard assessment of 4,10-dinitro-2,6,8,12-tetraoxa-4,10-diazaisowurtzitan (TEX) by accelerating rate calorimeter (ARC)," *J. Therm. Anal. Calorim.*, vol. 126, pp. 467–471, 2016.
- [19] D. Townsend and J. Tou, "Thermal hazard evaluation by an accelerating rate calorimeter," *Thermochim. Acta.*, vol. 37, pp. 1–30, 1980.
- [20] H. Peng and W. H. Chen, "Thermal decomposition kinetics of urotropin," *Chinese Journal of Energetic Materials*, vol. 24, no. 5, pp. 497–502, 2016.
- [21] S. Zhao and W. F. Pu, "Thermal behavior and kinetics of heavy crude oil during combustion by high pressure differential scanning calorimetry and accelerating rate calorimetry," *Journal of Petroleum Science and Engineering*, vol. 181, 2019.
- [22] AKTS. (2013). AKTS-Thermokinetics and AKTS-Thermal Safety Software. [Online]. Available: <http://www.akts.com>; Advances Kinetics and Technology Solutions.

Copyright © 2020 by the authors. This is an open access article distributed under the Creative Commons Attribution License which permits unrestricted use, distribution, and reproduction in any medium, provided the original work is properly cited ([CC BY 4.0](https://creativecommons.org/licenses/by/4.0/)).



**Jun Zhang** is a Ph.D. student majoring in mechanical engineering at Nanjing University of Science & Technology. He was studying on thermal hazard of the process of synthesizing energetic materials and investigating the thermal decomposition characteristic and kinetics of DINA, RDX, HMX and HMT, etc. His research interests are in the areas of process thermal safety and risk assessment.



**Yingying Ma** received the master's degree in chemical engineering from the Germany University. She is currently a process safety engineer at Solvay (China) Co., Ltd. Her research interests are in the areas of process thermal safety research and risk assessment, pressure relief design and optimization.



**Shuxin Chen** received her master's degree in safety science and engineering from Nanjing University of Science & Technology. She is currently a chemical engineer at Shanghai Chemical Industry Research Institute. Her research interests are in the areas of hazardous chemicals transportation classification and identification.



**Liping Chen** received the Ph.D. degree in mechanical engineering from Nanjing University of Science & Technology. She is currently a professor with the Department of Safety Engineering at Nanjing University of Science & Technology, China. Her research interests are in the areas of process thermal safety and risk assessment.



**Wanghua Chen** received the Ph.D. degree in weapon safety technology engineering from Nanjing University of Science & Technology. He is currently a professor with the Department of Safety Engineering at Nanjing University of Science & Technology, China. His research interests are in the areas of process thermal safety and risk assessment and explosion safety design and protection.